

Layer Formations in Electron Beam Sintering

M. Kahnert, S. Lutzmann, M. F. Zaeh

iwb Institute for Machine Tools and Industrial Management, Technische Universitaet Muenchen, Germany

Abstract:

Among direct metal processing manufacturing technologies (Rapid Manufacturing), Electron Beam Sintering (EBS) exhibits a high application potential. Especially, the fast beam deflection provided by electromagnetic lenses allows the realization of considerable building speeds and minor residual stresses. Therefore, this paper aims to examine and utilize the given potential for additive layer manufacturing. In this context, the deployed scanning strategy is a very important aspect. By means of an increasing computer power, innovative and flexible patterns for the solidification of the powder can be implemented. Thus, different patterns are being examined and evaluated. Finally, occurring effects in the exposed zone are introduced.

Introduction

Due to the trend in direct manufacturing of high-quality metal goods, the importance of the corresponding additive layer manufacturing process is increasing. It is therefore essential, to reliably produce parts with defined requirements like density, stiffness or hardness. This especially includes parts, which are exposed to high strains or must fulfil high demands concerning lightweight construction.

Up to now, the additive layer manufacturing of metal parts was dominated by the use of laser beam systems [1]. Despite to the advantages of the additive layer manufacturing technologies [2]. Restrictions exist for the laser based systems regarding the use of different metal materials, the achievable building speed and the porosity of the parts. For example, especially the mirror galvanometers are limiting the process. First, the restricted thermal capacitance of the mirrors is restraining the applicable beam power. Second, a high inertia of the mirrors within the scanning system prevents that the track accuracy is adhered adequately also by a high scanning speed [3]. As a result, the economic use of high-alloyed metals (e.g. tool or stainless steel) is limited. This prohibits a more extensive use of additive layer manufacturing technologies for example in the aerospace industry or the medical technology. It is necessary to solve the described difficulties to establish the additive layer manufacturing technologies for an industrial use. The electron beam as an energy source for the selective melting of powder materials is therefore a promising approach [2, 4].

State of the art

The electron beam technology has been established in nearly all metal processing and in a number of other areas. Electron beam generators can possess a power reaching from several Watts up to some hundreds of Kilowatts [5]. They are used for electron-microscopy (low power), for vaporization systems (high power) and for non-thermal processes. Commonly manufacturing technologies, applying an electron beam are assigned to the group joining (e.g. eb-welding),

machining (e.g. eb-drilling), coating (e.g. eb-coating) and the change of material properties (e.g. eb-hardening). Furthermore, the improved beam guide enables, together with the increasing computer technology, the control of the beam deflection up to 50 MHz. It is therefore possible to realize complex beam deflection figures [6, 7].

In the area of the additive layer manufacturing the idea of using the electron beam as an energy source was pursued. In particular, it had the objective to increase the building speed and to use alternative materials. The disadvantages of the laser based technologies should be compensated by that approach. The basic procedure of Electron Beam Sintering (EBS) is similar to the laser based technologies. The process sequence (lowering the building platform - powder deposition – sintering of powder) does not differ much from other additive layer manufacturing technologies which are selectively melting powder materials, as shown in Figure 1.

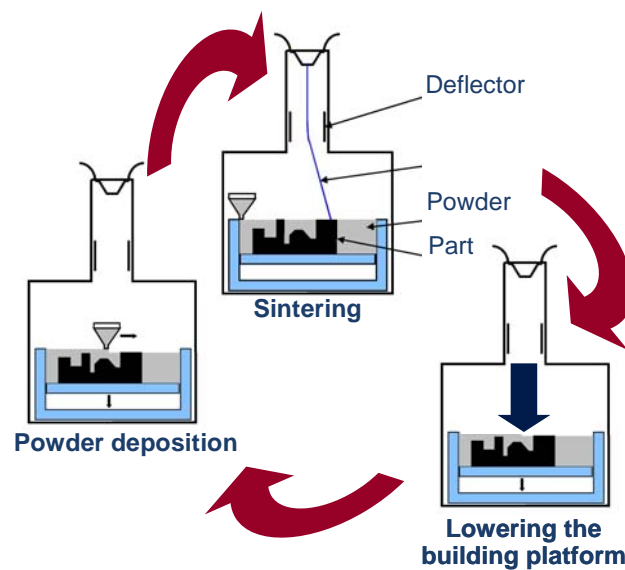


Figure 1: Functional principle of Electron Beam Sintering (EBS)

First papers with a description of the electron beam as an energy source for direct manufacturing were published in 1992 [8]. In 1997, patents led to the foundation of the Swedish company ARCAM. ARCAM as an equipment manufacturer distributes the two systems EBM S12 and A2 [9]. Tamminger et al. [10] and Dave [11] suggested the use of wire feed systems to produce parts with the electron beam. Another research approach was published by Qui et al. [12].

A commercial electron beam generator with a vacuum chamber was modified by the *iwb* for the use as an additive layer manufacturing process. The system is provided by the company *pro-beam*, which is an equipment manufacturer as well as a contract manufacturer within the field of electron beam technology [3].

Use of an electron beam welding system

A schematic view of the system used for the experiments is displayed in Figure 2, which had been installed at the *iwb* site in 2004:

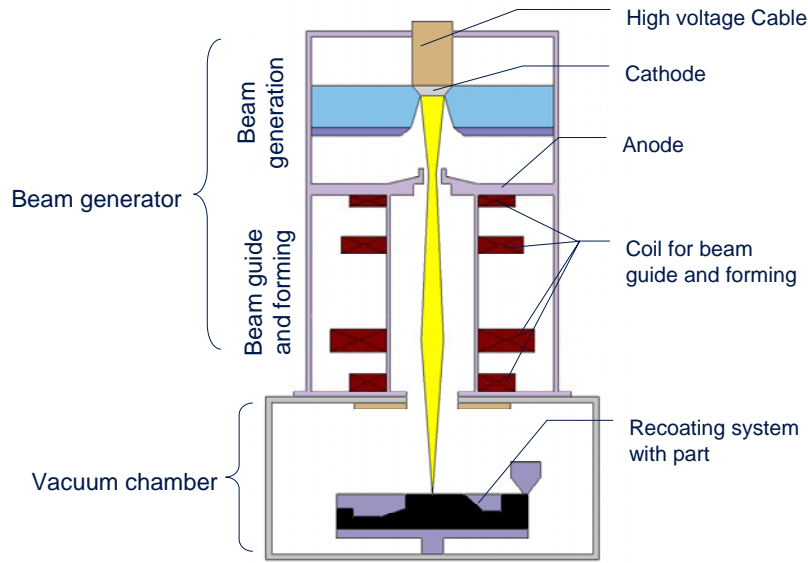


Figure 2: Schematic view of the applied electron beam system

The presented system is provided by the manufacturer usually for eb-welding of metallic parts [13]. The electron beam is produced within the beam generator. The beam is formed, focused and deflected by electromagnetic lenses. The high voltage, the so called acceleration voltage, which is applied between cathode and anode, accelerates the electrons towards the part located in the vacuum chamber. The acceleration voltage (up to 100 kV) is formed within a separate high-voltage generator.

The parameter setting, for example of the acceleration voltage, the beam current, the beam spot diameter and the beam deflection, is done by the integrated CNC- and PLC-system. They are addressing the electromagnetic lenses together with the beam control within a rate of 50 MHz. Thus, high scanning speeds of the beam focus can be realized. The evacuation of the process chamber is realized by a multistage system of several mechanical and diffusion pumps.

Transient physical effects requiring a preheating step

In contrast to laser beam sintering, the EBS process does not utilize photon radiation in order to solidify the powder bed. In fact, the electron beam is also referred to as a corpuscular ray consisting of moving charge carriers which possess a known inertia [14]. As a matter of principle, among various advantages concerning the process capability, this fact also leads to transient physical effects, such as the sudden spreading of the powder, as shown in Figure 3.

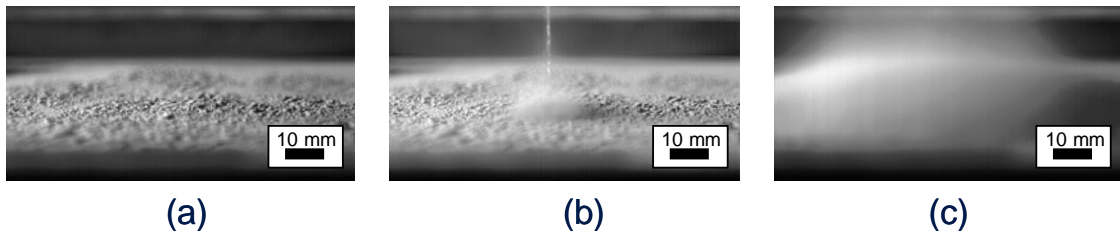


Figure 3: Spreading of one powder layer: (a) right at the activation of the electron beam, (b) after 0.005 s and (c) after 0.01 s [3]

The pictures have been recorded by a high-speed camera, whereby (a) the electron beam hits a 0.2 mm thick layer of lose H11 metal powder (X 38 Cr Mo V 5-1) at room temperature. Without transmitting any thermal energy into the material, the electron beam suddenly causes the uncontrolled acceleration of the powder particles in the near surrounding of the point of impact (b). In the right hand side picture it can be observed, that all the powder on the building plate is moving already after 0.01 s (c). The particles obviously interact in the course of the process, due to the fact that the beam has not been manipulated in power or location between the photographs (a) and (c). This effect has an extremely negative impact on the further course of the process, because all powder is removed from the building plate. The solution and elimination of this effect is the most important requirement towards the further development and industrial acceptance of the EBS process. The described effect has been addressed in previous publications [12, 15]. Sigl et al. [16] identify three different causes for the spreading of the powder. Starting with water residues in the powder, then momentum transfer into the powder, as well as electrostatic charge. The authors examine the listed effects and show, that water residues and momentum transfer are not relevant concerning the appearance of the spreading.

Based on this knowledge, the approach considering electrostatic charging is being investigated in more detail and extended by an electromagnetism theory. Thus, besides the repulsion of particles of corresponding charge, also forces due to the movement of electrons will be considered. The resulting force on the charged powder particles concurs with the study of the high-speed photographs (Figure 3), whereby the powder is being hurled primarily in the vertical direction as the electron beam is activated. Subsequently, it is not changed in its location and the amount of beam power is kept at a constant value. The movement of electric charged carriers leads to the generation of electromagnetic fields [17]. Assuming a current carrying conductor, the amount of the magnetic field H outside the conductor ($r \geq R$) can be determined local-dependent and time invariant by using the following equation [17]:

$$H(r) = \frac{I}{2\pi r} \quad (1)$$

In this equation, R describes the radius of the conductor respectively of the beam spot and I depicts the beam current. The amount of the magnetic field is subject to a rotation symmetric distribution. When $r = R$, the maximum amount of the magnetic field is reached. As in the above experiments (see Figure 6), the beam current is chosen equal to 14 mA, whereby the electric current density is assumed constant over the cross-section. In this case, the magnetic flux density

$$B = \mu_0 * \mu_r * H = 28 \mu\text{T} \quad (\mu_0 * \mu_r: \text{magnetic permeability equals } 4 * \pi * 10^{-7} \frac{\text{Vs}}{\text{Am}} \text{ [17]}).$$

The magnetic field then applies a force on the moving electric charges, the so called Lorentz force [17]:

$$\vec{F}_L = q * (\vec{E} + \vec{v} \times \vec{B}) \quad (2)$$

According to this equation, it results from the electric field \vec{E} , from the velocity \vec{v} of a charge q and the magnetic flux density \vec{B} . As an electric field \vec{E} only appears when a transient electron flux is given, $\vec{E} = 0$ and the resulting Lorentz force \vec{F}_L equals $q * \vec{v} \times \vec{B}$. According to the “Right-Hand Rule”, its direction is perpendicular to the lines of the magnetic flux as well as to the direction of the charge movement (see Figure 4):

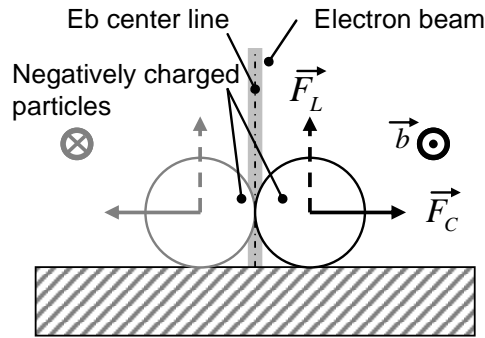


Figure 4: Lorentz force on negatively charged powder particles

Sigl et al. [16] have shown, that the electron beam transmits negative charge into the powder bed. If the electric resistance between the powder particles as well as between the powder bed and the building plate is too high, adjacent particles are being charged correspondingly. Thus, a Coulomb force of $2.426 \cdot 10^{-6}$ N emerges, which is clearly greater than the normal force of a powder particle ($1.09 \cdot 10^{-12}$ N) and leading to its acceleration along the building plate. Subsequently, they cross the lines of magnetic flux, whereby a force vector \vec{F}_L is being generated. According to Sigl et al. [16], a particle affected by the electron beam disposes an electric charge of $q = 9.8 \cdot 10^{-11}$ C. As it can be seen in Figure 3 (b), all powder grains in the surroundings of the point of beam impact are in movement already after 0.005 s. Therefore, the initial velocity of a powder particle is estimated to approximately 10 m/s from the photographs in Figure 3. On the assumption, that a particle first reaches a specific velocity before it is affected by the magnetic field, the resulting Lorentz force can be approximated as follows:

$$\vec{F}_L = q * \vec{v} \times \vec{B} = 2.74 * 10^{-11} \text{ N} \quad (3)$$

Hence, it was shown that the amount of resulting Lorentz force is of multiple magnitudes greater than a powder particle's gravitation force. Therefore, the particles are exposed to a considerable acceleration leading to an enormous hurling of the powder bed.

In order to reduce these transient physical effects, Sigl et al. [16] propose the following counteractive measures (see Figure 5):

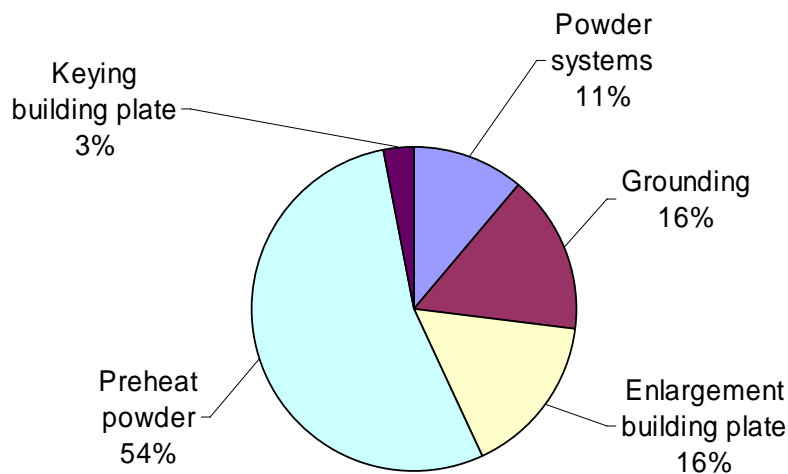


Figure 5: Estimation on the impact of the counteractive measures

Preheating the powder before its solidification has the greatest influence on the avoidance of the spreading effect. By increasing the powder bed temperature it can be achieved that single particles converge [18] and start to build up an electric conduction towards the grounded building plate. Thus, the influence from the electron beam does not lead to any electrostatic charging of the powder particles and therefore no Coulomb force arises. Furthermore, mechanical tie-ups build up, keeping the particles in place even in the event of any forces on the powder.

Based on the illustrated interrelations between the charging, magnetic fields and the spreading of the powder, the EBS process differs by the additional preheating step from laser-based processes. Hence, it consists of the following three steps (see Figure 6) [3]:

- powder deposition
- preheating of the powder
- scanning of the powder

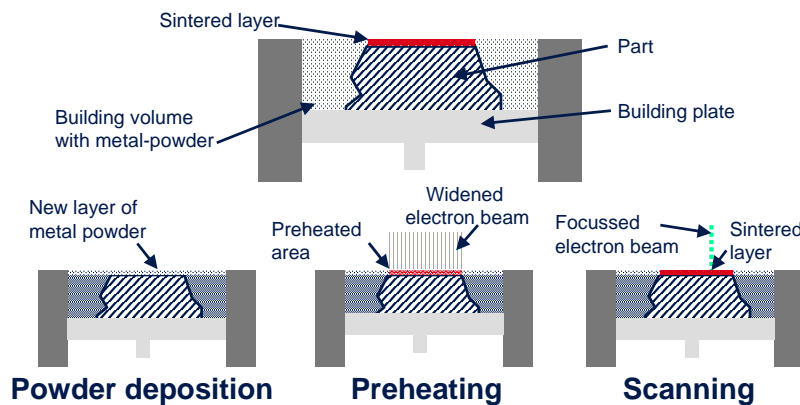


Figure 6: EBS process: powder deposition – preheating – scanning

During preheating, a defocused beam configuration is chosen in order to ensure a consistent energy input, until the powder has reached a temperature close to its melting point. From this point, the scanning process step can be initiated in order to selectively solidify the material. For both process steps, the utilized computer control provides adequate patterns for the beam deflection. In comparison to laser-based technologies, a considerably higher deflection frequency can be achieved by using electromagnetic lenses. Therefore, novel scanning patterns and melting strategies can be applied.

Scanning

Because of the described physical effects and the resulting preheating step the result of the selective sintering of the powder layer has to be analyzed under the influence of this preheating step. Furthermore, the parameters with the most significant influence are the beam current, the scanning pattern and the energy density within the molten zone. These parameters are investigated in the following. The tool steel H11 was used to carry out the experiments.

The essential correlation between pre-heating beam current and scanning beam current can be seen in Figure 7. This diagram shows the minimum of the necessary beam power to establish the

process within a molten zone. It is shown, that with an increasing preheating energy, and there with the temperature of the powder bed the required focussed beam power and current respectively is decreasing.

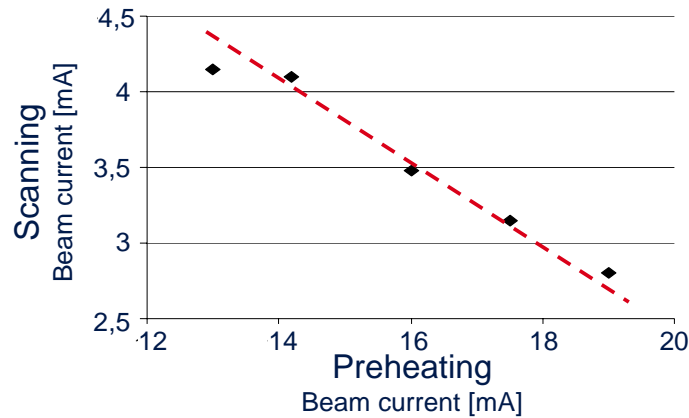


Figure 7: Relation of the beam current between preheating and scanning

This diagram indicates that the utilized beam current must be considered within the choice of the parameters. For the following investigations a constant preheating energy of $P = 1,6 \text{ kW}$ was used. Thus, all beam values must be seen in dependence of this preheating energy.

Among the singular examination of the beam current, the experiments must be considered under the consideration of other parameters, like for example the energy density (J/mm^3). That describes the inserted beam energy into the layer after the preheating. It is derived by the parameters scanning speed, layer thickness, and hatch distance [19]:

$$\text{energy density} = \frac{\text{electron beam power}}{\text{scanning speed} * \text{hatch distance} * \text{layer thickness}}$$

This value has a significant influence for example on the surface quality, which is rated in a scale from 1 (poor) up to 10 (good). This subjective rating is necessary, because it was not possible to measure the surface by a tactile surface measuring apparatus for probes with a poor quality (see Figure 8).

Figure 8 also shows, that for a part with a good surface quality an energy density between $1 \text{ J}/\text{mm}^3$ up to $2.5 \text{ J}/\text{mm}^3$ is necessary. If an energy density above $2.5 \text{ J}/\text{mm}^3$ is used, the maximum surface quality possible declines. This is underlined by a curve in the diagram. The major reason for the declining surface quality is the increased appearance of pores.

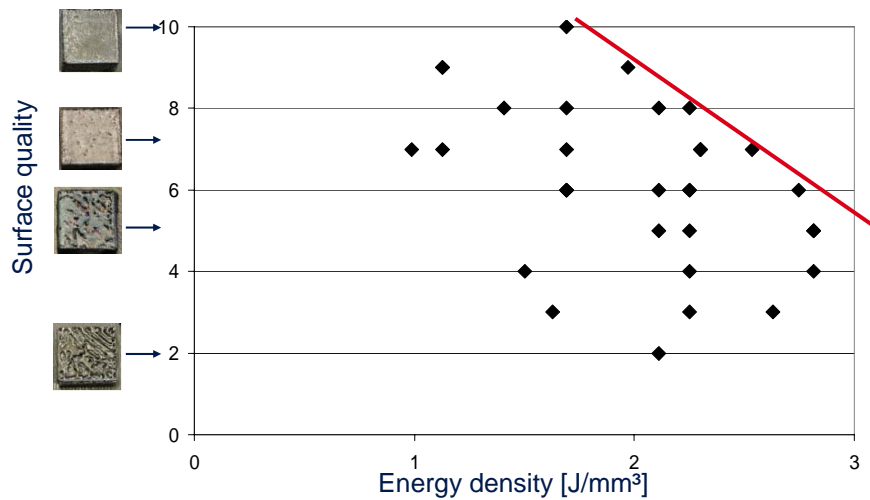


Figure 8: Effect of the energy density on the surface quality

The cohesion of the different layers is mainly influenced by the energy density as well as the scanning pattern of the hatch. In Figure 9 results of different scanning strategies can be seen. The beam was deflected in x-direction (x-Hatch) as well in x and y direction alternating in every layer (xy-Hatch alternating) and in x and y-direction in every layer (xy-Hatch). The photographs of the parts are showing, that in particular the x-hatch leads to high residual stress within the different layers. These residual stresses are emerging during the cooling of the melted metal in the layer and are causing the borders of the part to bend up. Hence, gaps between the layers are leading to an insufficient layer cohesion. The gaps can be seen most notably in the left photography of Figure 9.

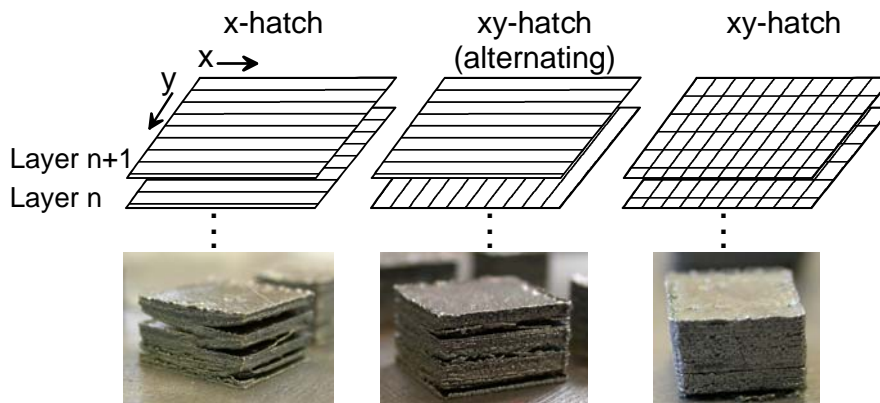


Figure 9: Effect of scanning strategies on the layer connection

As mentioned, the cohesion of the layers is controlled by the energy density. In Figure 10, the grade of the layer connection in correlation of the energy density and the scanning pattern is shown. The grade of the layer connection is quoted likewise from 1 (poor) up to 10 (good). In the diagram, it is shown that an increasing energy density within the molten zone improves the connection of the layers. Furthermore, this diagram underlines the relevance of the scanning strategy. As described, the scanning strategy, which causes the fewest amount of residual stresses

leads to a good cohesion. Because of the most uniform energy input the best results can be received from the xy-hatch

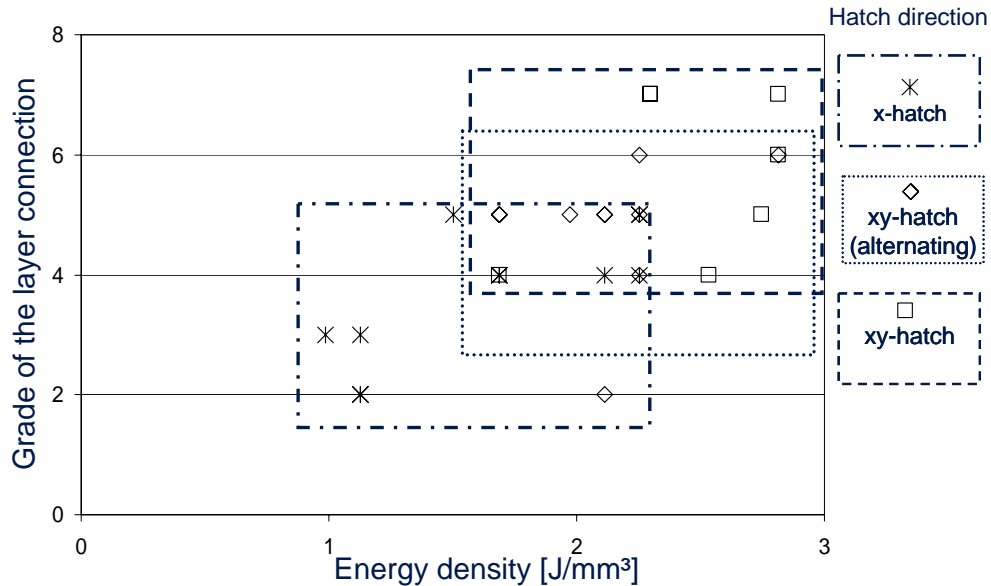


Figure 10: Effect of the scanning strategy and the energy density on the layer connection

The described interrelations emphasize that the examined parameters cannot be considered individually. For example, a high energy density is needed to achieve a good connection between the layers, but it also causes poor surface qualities. For a further development of the electron beam sintering it is required to consider the energy density as well as other electron beam and process parameters as relevant. The basic interdependency between these parameters must be elaborated before establishing a stable process.

Effects during scanning

By means of visual observation of the EBS process, the dependence on the energy density could also be demonstrated. In Figure 11, a chronological sequence from a high speed camera of the x-hatch melting of the layer surface is displayed. Energy with the density of 1.13 J/mm³ was inserted into the square (edge length 12 mm) during scanning. The square was solidified by tracing the electron beam on different lines. This led to the melting of the layer surface which is displayed in that recording. During the scanning of the first line the melting only occurs at the focused beam spot and the immediate area of melting can be seen. No enlargement of that zone can be recognized. The focused beam spot is more visible in the photos of the other lines, because scanning lines are overlapping and a bigger area of melting is caused. The pictures of the lines 21 and 75 are also showing that the molten zone only affects the surrounding powder marginal. The electron beam spot is indeed getting bigger, but the specific powder characteristics (e.g. low heat conductivity) prevent an enlargement of the molten zone.

The pictures also demonstrate that this energy density leads to a good surface quality.

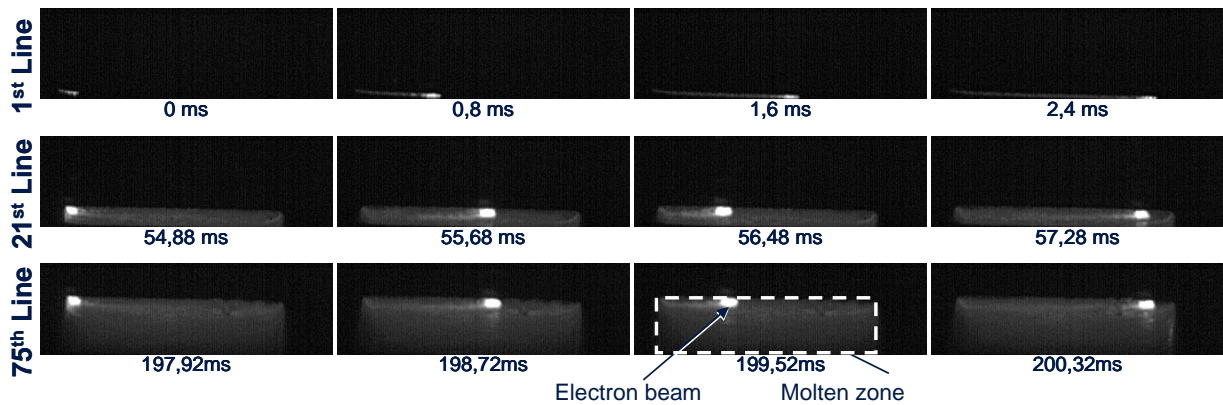


Figure 11: Recording of the sintering of one layer with the energy density of 1.13 J/mm^3

On the other hand, the pictures in Figure 12 were realized by recording the sintering of one layer with the energy density of 2.82 J/mm^3 .

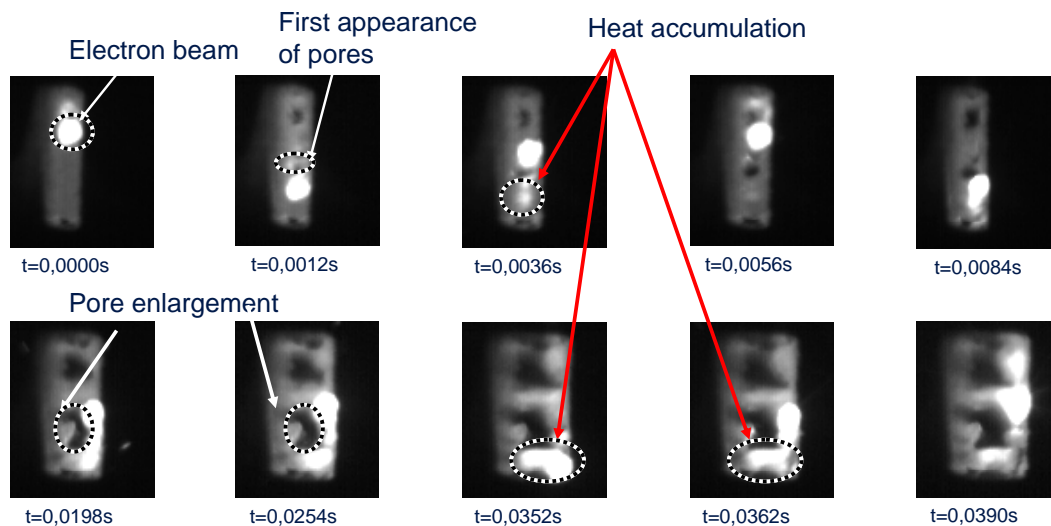


Figure 12: Recording of the sintering of one layer with the energy density of 2.82 J/mm^3

Therefore, the powder not only melts, but the surface tension causes the liquefied material to form balls. In consequence, it leads to a local heat accumulation and thus to pores. This inhomogeneity of the heat distribution is getting bigger while the scanning of the beam focus carries on. So the accumulation of material and the pores within the square are getting successively bigger. After stopping the heat input the molten material solidifies. Resulting humps from material accumulations can reach above the layer surface. This not only leads to a poor surface quality. It can also cause the rake mechanism of the recoating system to stop, so that the process itself has to be aborted.

Conclusion

The presented investigations have shown that the fast beam deflection enables the selective sintering of metal powders with the electron beam. Using different beam patterns metal parts could be produced. Nevertheless, transient physical effects require an adjusted process. Due to occurring electrostatic and magnetic forces the metal powder is spreading in an uncontrolled way. Therefore, the conventional process has to be extended by an additional preheating step. During that step the powder is heated in a gradual manner by a defocussed electron beam.

The preheating determines the result of the following sintering step. By using a considerable preheating energy the required beam power for scanning can be decreased. Furthermore, the energy density has a great influence on the process result. On the one hand, it determines the surface quality. On the other hand, a minimum amount of energy is necessary for the connection of subsequent layers, as well as the applied scanning strategy. Scanning strategies causing a high thermal gradient result in high residual stresses and delaminating of melted layers. The described effects could be investigated as well with high-speed camera recordings. Defects like pores and humps could be observed when using high energy density.

For the further process development it is vital to examine all occurring effects and to optimize the process in a holistic manner. Also, adapted scanning strategies need to be developed and their influence on the process results evaluated.

References

- [1] Zäh, M. F.; Sigl, M.; Seefried, M.; Hagemann, F.; Kahnert, M.; Müller, A.; Meindl, M.: Wirtschaftliche Fertigung mit Rapid-Technologien: Anwender-Leitfaden zur Auswahl geeigneter Verfahren. 1st Edition. Munich: Carl Hanser 2006.
- [2] Meindl, M.: Beitrag zur Entwicklung generativer Fertigungsverfahren für das Rapid Manufacturing. Diss. Technische Universität München (2004). Munich: Utz 2005. (iwb Forschungsberichte 187).
- [3] Zäh, M. F.; Kahnert, M.: Den Elektronenstrahl für das selektive Sintern von metallischen Pulvern nutzen. In: Meyer, R. (Ed.): Euro-uRapid2006; Frankfurt/Main 27.-28.11.2006. Frankfurt/Main: Fraunhofer-Allianz Rapid Prototyping 2006, pp. B2/3.
- [4] Lutzmann, S.; Kahnert, M.; Sigl, M.: Elektronenstrahlsintern als Zukunftstechnologie im Rapid Tooling. In: Zäh, M. F. et al. (Ed.): Rapid Manufacturing: Heutige Trends-Zukünftige Anwendungsfelder; Augsburg 6.7.2006. Munich: Utz 2006, pp. 7-1 - 7-26. (iwb Seminarberichte 81).
- [5] Bartel, R.: ELEWER – Der Elektronenstrahl als Werkzeug. Dresden: Fraunhofer-Institut für Elektronenstrahl und Plasmatechnik (FEP) 2002.
- [6] Dobeneck, D.; Löwer, T.; Adam, V.: Elektronenstrahlschweißen: das Verfahren und seine industrielle Anwendung für höchste Produktivität. 1st Edition Landsberg/Lech: Moderne Industrie 2001. (Die Bibliothek der Technik 221).
- [7] Dobeneck, D. v.: Elektronenstrahl-Schweißen: Anwendungsbeispiele aus 30 Jahren Lohnschweißpraxis. Planegg: pro-beam 2004.

- [8] Patent WO 1994026446 A1 (24.11.1994). Larson, R. Pr.: SE 9301647 (12.05.1993). Larson, R.: Method and Device for producing Three-dimensional Bodies.
- [9] ARCAM: APPLICATIONS. <<http://www.arcam.com/applications/index.asp>> - 5.6.2007.
- [10] Taminger, K. M. B.; Hafley, R. A.: Characterization of 2219 Aluminium Produced by Electron Beam Freeform Fabrication. In: Bourell, D. L. et al. (Ed.): Solid Freeform Fabrication Symposium Proceedings 13; Austin, Texas/USA 5 - 7.8.2002. The University of Texas at Austin 2002, pp. 482-489.
- [11] Davé, V. R.: Electron Beam Assisted Materials Fabrication. Diss. Massachusetts Institute of Technology (MIT) (1995).
- [12] Qi, H. B.; Yan, Y. N.; Lin, F.; He, W.; Zhang, R. J.: Direct metal part forming of 316L stainless steel powder by electron beam selective melting. Proceedings of the Institution of Mechanical Engineers -- Part B -- Engineering Manufacture 202 (2006) 11, pp. 1845-1853.
- [13] pro-beam: Dokumentation iwB: Bedienerhandbuch. Planegg: 2004.
- [14] Dobeneck, D.; Löwer, T.; Mehnard, C.: Entwicklungspotenziale der thermischen Materialbearbeitung mit Elektronenstrahlen im Vergleich zu Laserstrahlen. In: Sepold, G. et al. (Ed.): Laserstrahlfügen : Prozesse, Systeme, Anwendungen, Trends ; Beiträge zum 4. Laser-Anwenderforum Bremen; 12.-13.9.2002. Bremen: BIAS-Verlag 2002, pp. 35-44. (Strahltechnik 19).
- [15] Sigl, M.: Entwicklung von Rapid-Technologien am Beispiel des Elektronenstrahlsinterns. Diss. Technische Universität München (publication follows)
- [16] Sigl, M.; Lutzmann, S.; Zäh, M. F.: Transient Physical Effects in Electron Beam Sintering. In: Bourell, D. L. et al. (Ed.): Solid Freeform Fabrication Symposium Proceedings 17; Austin, Texas/USA 14. - 16.8.2006. The University of Texas at Austin 2006, pp. 397-405.
- [17] Stöcker, H.: Taschenbuch der Physik : Formeln, Tabellen, Übersichten. 3rd Edition Thun: Deutsch 1998.
- [18] German, R. M.: Sintering theory and practice. New York: Wiley 1996.
- [19] Kruth, J. P.; Kumar, S.; Vaerenbergh, J. V.: Study of laser-sinterability of ferro-based powders. Rapid Prototyping Journal 11 (2005) 5, pp. 287 - 292.